UDC 66.081.4:546.492:661.691.32

DOI: 10.15372/CSD2022393

EDN: DQBMNA

Sorption Purification of Selenous Acid Solutions from Mercury

A. A. KOROLEV[1], V. A. SHUNIN[1], K. L. TIMOFEEV[1,2], G. I. MALTSEV[1], R. S. VOINKOV[1]

[1]JSC "Uralelectromed", Verkhnyaya Pyshma, Russia
E-mail: V.Shunin@elem.ru

[2]UMMC Technical University, Verkhnyaya Pyshma, Russia

(Received 21.01.22; revised 14.03.22)

Abstract

As an alternative to mercury release by cementation on metallic aluminum, for the purpose of improving the purity of commercial selenium, we investigated the processes of selective sorption of mercury ions from the technological solutions of selenous acid onto styrene-divinylbenzene Lewatit MP 68 resin. The isotherms of mercury ion sorption are obtained, the main quantitative parameters and limiting stages of the process are assessed. It is established that for a low degree of resin filling with the sorbate (with the equilibrium concentration of mercury ions in solution ≤0.4 mmol/dm^3) and for the sorbent – sorbate type interaction, the distribution coefficient decreases initially, and then increases while the sorption ability increases and the structures of sorbate – sorbate type are formed. The degree of mercury extraction from solution (β) is inversely proportional to the equilibrium concentration of mercury ions in the solution (C_{eq}) and is described by the linear equation: $\beta = -133.5C_{eq} + 99.81$. Experimental data processing shows the simultaneous occurrence of the stages of external (film) and internal (gel) diffusion, which is evidence in favour of mixed diffusion sorption mode. The rate constants of external diffusion are approximately three times larger than the rate constants of internal diffusion. It is shown that the kinetic equations of pseudo-first and pseudo-second order models provide satisfactory description of experimental data, and that the difference between determination coefficients is not large ($R_i^2 > 0.98$). The values of thermodynamic functions of mercury sorption within the temperature range 298–333 K were determined: $-\Delta G$ = 2.35–2.99 kJ/mol, ΔH = 3.1 kJ/mol, ΔS = 18 J/(mol · K). The practical significance of the revealed sorption parameter (dynamic exchange capacity of Lewatit MP resin is 68–269 g/dm^3, specific volume of solution for resin saturation in the dynamic mode is 3800, element content in saturated resin is, %: Hg ~26.0, Se <1.0) is due to their involvement in designing the industrial installation.

Keywords: selenium, mercury, ion exchanger, solution, sorption, desorption, degree of extraction, diffusion, distribution coefficient, concentration, isotherm

INTRODUCTION

The production of technical-grade selenium at the JSC Uralelektromed (Verkhnyaya Pyshma) from the raw material and intermediate products of lead, zinc and sulphuric acid production (selenium-mercury sludge, selenium-arsenic cakes, *etc.*) resulted in the product with increased concentration of mercury, which is a difficultly refinable impurity. Leaching of metallurgical dust gives the solutions of selenous acid with the composition, g/dm^3: H^+ 2–3; Se 100–180; Hg^{2+} ~1.0; Te 0.03–0.2; As 1.1–1.7, which are to be purified from mercury to the residual concentration not higher than $1 \cdot 10^{-3}$ g/dm^3 for obtaining selenium of the

© Korolev A. A., Shunin V. A., Timofeev K. L., Maltsev G. I., Voinkov R. S., 2022

necessary grade. This defines the relevance of the present work.

Among the existing methods of solution purification from mercury, electrochemical reduction of the element is to be mentioned first of all: more than 92 % of mercury is removed in the form of Hg−allow within 150 min, with the current efficiency ~75 %. After electrodeposition, mercury in the spent cathode maybe processed by thermal desorption [1]. The application of synthesized microporous materials based on the silicates of niobium (AM-11) and vanadium (AM-14) is known. The experimental data for AM-11 (deviation 3.58 %, determination coefficient R^2_{adj} = 0.980, likelihood function AIC = 52.8) were described with higher reliability with Langmuir isotherm, predicting the maximal absorption of mercury 161 mg/g, which corresponds to the level of the best ion-exchange materials, while the data for AM-14 were in better correspondence with Temkin model (deviation 3.92 %, R^2_{adj} = 0.985, AIC = 54.2) [2].

A combined electron beam and adsorption method of purification from Hg(II) is based on the synergistic effect of the joint action of irradiation and sorbent − the materials of plant origin. For instance, after the addition of cellulose, carboxymethylcellulose, starch, wheat flour into water, irradiation with the electron beam follows, then precipitation and filtration of the additives with absorbed mercury. The method is based on the synergistic effect of irradiation and sorbent. In particular, the addition of 25 mg/dm^3 of flour into water containing 1 mg/dm^3 Hg(II), and irradiation with the dose of 1.1 kGy with an inert gas passing through the system resulted in Hg(II) removal by 98 % [3]. Efficient and cheap adsorbents are obtained through an increase in the surface area of the materials and by doping with heteroatoms. Sulphur-doped activated carbon is superior to commercial activated carbon in mercury absorption: possessing high specific surface area (1329 m^2/g) and sulphur content up to 14.8 wt. %, optimal porous structure, low cost and convenience for recovery, this material demonstrates high absorption capacity with respect to mercury (187 mg/g) [4]. The alkaline sorbent and active centres based on chalcogen were chosen to implement inductive adsorption of HgO. It has been demonstrated that the composite ZnO−CuS with the optimal molar ratio 4 : 3 captures HgO efficiently. Copper (II) sulphide was the leading active centre for HgO adsorption using the surface S_n^{2-} ions. Surface sulphation occurred, a part of HgO was adsorbed with the formation of HgS and $HgSO_4$ [5]. To remove elemental mercury Hg^0, magnetospheres (S-MS) separated from fly ash and modified with the help of H_2S were used as an efficient sorbent. Elemental sulphur with a high affinity to Hg^0 was formed on the surface of S-MS through selective catalytic oxidation of H_2S. The efficiency of adsorption on S-MS was more than 80 % Hg^0 at sulphidation temperature 150 °C for 30 min. Magnetospheres S-MS may be used through injection into the channel before the system of wet electrostatic precipitator (WESP) [6, 7]. After thermal treatment and application of plasma method [8], mercury may be desorbed from the adsorbents, and their activity may be recovered. At the same time, mercury may be purified with the help of a chelating agent, acid washing and electrolysis, this providing the possibility to use the metal. Efficient photocatalysts modulate the heterojunction $CeO_2/ZnIn_2S_4$ according to Z-scheme for the photocatalytic oxidation of Hg^0. Due to the strong synergistic effect between the large specific surface, heterojunction according to Z-scheme and oxygen vacancies, the optimized photocatalyst demonstrates mercury removal at a level of 86.7 % [9].

A platform for mercury removal has been developed for solar evaporators. It is based on synthesized polysulphide nanoparticles (PSNS). The use of PSN-functionalized aerogel evaporator with reduced graphene oxide (PSN-rGO) leads to high evaporation rate 1.55 kg/(m^2 · h) with energy efficiency equal to 90.8 %. Possessing the advantages of interconnected porous structure and adsorption capacity, the photothermal aerogel provides complete purification of wastewater from heavy metal ions [10].

Mercury cementation ($HgCl_4^{2-}$) in chloride medium involving metal zinc, iron and aluminium as reducing agents is known. The reaction order was 1.08±0.05 with respect to mercury concentration. An optimal solution pH value was determined for each metal under investigation: 4.0−5.0 for zinc, 3.0 for iron, and 3.0−4.0 for aluminium. Tests with metal particles characterized by different grain sizes in different doses showed that the specific surface area and mass of a metal are important parameters for mercury removal. Optimal conditions determined for synthetic mercury solutions were tested using the real mercury filtrate. It is shown that it is possible to obtain 0.08 ‰ ($8 \cdot 10^{-2}$ g/dm^3) mercury in the resulting solution [11].

In the acid solutions of gas trapping in the presence of sulphur oxides, the interaction of mercury with SO_2 cannot be excluded, resulting in the formation of very strong complexes $[Hg(SO_3)_2]^{2-}$ (instability constant $K_{inst} = 2.19 \cdot 10^{-23}$); $[Hg(SO_3)_3]^{4-}$ ($K_{inst} = 1.45 \cdot 10^{-23}$); $[Hg(SO_3)_4]^{6-}$ ($K_{inst} = 1.45 \cdot 10^{-23}$) [12]. The presence of SO_2 and SO_3 in solution has a substantial effect on the adsorption capacity of the sorbent based on carbon with respect to mercury [13]. Sulphur copolymers containing micro- and macroporous structures actively interact with mercury compounds in solution [14]. At a temperature of 296 and 348 K, the presence of multinuclear sulphide complexes Hg–S was revealed (4–370 parts per million Hg), where mercury is coordinated by two S atoms at a distance of 0.23 nm with the linear position [–S–Hg–S–] [15, 16]. The formation of $[PhHg(LH)]_n$ **1** is possible, where LH = 2-cyanoaminothiaaohenolate anion $(SC_6H_4NHC{\equiv}N)^-$; Ph = phenyl. The reaction of **1** with Ph_3P and Ph_3PS gives $[Hg(LH)_2(Ph_3P)_2]$, $[PhHg(\mu\text{-}LH)(Ph_3PS)]_2$, $[Hg(\mu\text{-}L)(PPh_3)]_2$ [17].

Additional presence of chloride ions makes the formation of complex compounds of mercury possible: $HgCl^+$ ($K_{inst} = 1.8 \cdot 10^{-7}$); $HgCl_3^-$ ($K_{inst} = 8.5 \cdot 10^{-15}$); $HgCl_4^{2-}$ ($K_{inst} = 8.5 \cdot 10^{-16}$) [18–20]. Anion nitrogenous heterocyclic carbine complexes of C,N-bound mercuramacrocycles $\{Hg_4Cl_4(R\text{-}Bim)_4\}$ (where BimH = benzimidazole; R = Ph, Py) are obtained in the reaction of N-substituted benzimidazoles with $HgCl_2$ [21]. The interaction of *o*,*o*′-dilithiuooctafluorobiphenyl with $HgCl_2$ leads to the formation of complex anion $\{[(o,o'\text{-}C_6F_4C_6F_4Hg)_4]Cl\}^-$ [22]. A complex of tris(*N*-methylimidazoline-2-selon) with mercury (II) has been described – $[(MeImSe)_3HgCl]^+Cl^-$ [23]. The reaction of mercury (II) chloride with triphenylphosphine (PPh_3) and pyrimidine-2-thion (pmtH) at the molar ratio of 1 : 1 : 1 gives $[Hg_2Cl_2(PPh_3)_2(pmt)_2]$ (pmt = pyrimidine-2-thion anion) [24]. The complexes of metal chloride (for the metals of zinc triad) with pyridazine of the type of $[M(pyridazine)Cl_2]_n$ (M = Zn(II), Cd(II), Hg(II)) are known, which are isostructural polymers of the formulas of catena[bis(μ_2-chloro)-(μ_2-pyridazine-*N,N*′)]mercury(II) [25].

Among the listed methods of solution purification from mercury, a promising one appears to be the sorption technology possessing a number of advantages, among which there are controllable degree of purification, compact equipment, reliability of operation and performance simplicity, stability against the concentrational and hydraulic variations.

The goal of the work was to choose a sorbent and the optimal process parameters for the purification of selenous acid solutions from mercury to the residual concentration not more than 1 mg/dm^3.

EXPERIMENTAL

Taking into account the presence of negatively charged mercury complexes in the solutions of selenous acid, for choosing the subsequent object of investigation we tested the samples of industrial sorbents differing from each other in nature, rendered by the Technolgocil Division of Uralelektromed JSC: synthesized anion-exchange resins – vinylpyridine VP-1П and VP-1AP, styrene-divinylbenzene Lewatit MP 68, activated coal of Haycarb and Goldcarb grades.

Component concentrations in the solution were determined in the certified central laboratory at Uralelektromed JSC using a two-ray atomic absorption spectrometer AA-7000 (Shimadzu, Japan) for plasma and electrothermal atomic absorption analysis according to analytical procedures described in the corresponding State Standards and technical specifications.

To evaluate the static exchange capacity of the sorbents under tests, weighted portions 3 and 5 cm^3 in volume were placed in flasks, and then the solutions were poured in the flasks: 100 cm^3, with the composition, g/dm^3: H^+ 5.0–5.2; Hg 0.027–0.046; Zn 2.8–3.7; Fe 0.3–0.6; As 0.16–0.2; Cu 0.03–0.06. The mixtures in the flasks were stirred for 72 h at room temperature to ensure the equilibrium in the system was established. Then the solution was separated from the sorbent, and mercury concentration was determined. On the basis of thus obtained results, the static exchange capacities (SEC, g/dm^3) for the sorbents under tests were determined according to equation

$$SEC = ((C_0 - C_{eq})V_{sol})/V_{sorb}$$

where C_0, C_{eq} are initial and equilibrium concentrations of Hg in solution, g/dm^3; V_{sorb}, V_{sol} are the volumes of the sorbent and the solution, respectively, dm^3 (Table 1).

The SEC values for the tested sorbents, except for VP-1P resin, are almost identical and for the weighted portions 3 and 5 cm^3 in volume are equal to 1.47–1.53 and 0.91–0.92 g/dm^3, respectively. However, for subsequent studies we chose Lewatit MP 68 (weakly basic macroporous anion-exchange resin with monodisperse granule size distribution; the ion form is a free base/Cl^-;

TABLE 1

Sorbent capacities of the sorbents with respect to mercury under static conditions

Sorbent	Sorbent volume			
	3 cm^3		5 cm^3	
	$[Hg^{2+}]$, mg/dm^3	SEC, g/dm^3	$[Hg^{2+}]$, mg/dm^3	SEC, g/dm^3
VP-1P	19	0.90	15	0.62
VP-1AP	1	1.50	<1	0.91
Lewatit MP-68	<1	1.53	<1	0.92
Haycarb	<1	1.53	<1	0.92
Goldcarb	2	1.47	<1	0.91

the functional group is tertiary/quaternary amine; swelling coefficient is 25 vol. %), which conserves high consumer properties and capacity with respect to mercury within 30 cycle sorption-desorption testing mode.

To build up the sorption isotherm, weighted portions of the sorbent, 0.2 g, were filled with 4–200 cm^3 of the model mercury solution (150 mg/dm^3) in sulphuric acid and kept for 3 h. The sorbent was separated from the solution by filtering, and residual mercury concentration in the solution was determined. Содержание Mercury content in the sorbent phase was calculated as the difference between the initial and residual element concentration in the solution. In some experiments, a sorbent portion of 10 mg was filled with 20 cm^3 of the model solution containing ~1.7 mg of mercury, and then the duration and temperature of sorption were varied, as well as the concentrations of mercury and sulphuric acid in the initial solution. In the experiments on mercury sorption under dynamic conditions, пропускали the initial solution 0.046–0.99 g/dm^3 Hg was passed through the weighted portion of 1–10 g of Lewatit MP 68 with the volume flow rate of v = 2–5 h^{-1}. The volume of solution fractions analyzed after sorption was 50–200 cm^3.

RESULTS AND DISCUSSION

Sorption process under static conditions is described by equations linking the amount of substance sorbed per unit mass or volume of the ion-exchange material, or ionite (sorbate) – Q_{sorb} or SEC, and the equilibrium concentration of the substance in the liquid phase (sorptive) – C_{eq}, taking into account chemical and geometric inhomogeneity of the sorbent and the properties of the sorbed substance. One of the characteristics is the distribution constant $K_{distr} = Q_{sorb}/C_{eq}$ (Table 2, Fig. 1).

Absorption of the anion complexes of mercury by Lewatit MP 68 sorbent allowed us to obtain a typical sorption isotherm (see Fig. 1, *b*), on which it is possible to distinguish the regions of equation applicability: I – Henry ($Q_{sorb} = K_{ads}C_{eq}$); II – Langmuir ($C_{eq}/Q_{sorb} = C_{eq}/Q_s + 1/(K_{ads}Q_s)$); III – Dubinin–Radushkevich ($Q_{sorb} = Q_s \cdot \exp[-(K_{ads}/\beta^2)(RT \ln(1 +$

TABLE 2

Results of the experiment on mercury recovery at different L/S values

V_{sol}/V_{sorb}	C_{eq}, mg (mmol)/dm^3	$\beta = (C_{in} - C_{eq})/C_{in}$, %	Q_{sorb} (SEC), mmol (g)/dm^3	$K_{distr} = Q_{sorb}/C_{eq}$
∞	150.0 (0.748)	0	–	–
1000	138.7 (0.691)	7.53	56.3 (11.29)	81.5
200	116.9 (0.583)	22.07	33.0 (6.62)	56.6
100	104.9(0.523)	30.07	22.5 (4.51)	43.0
67	98.9 (0.493)	34.07	17.0 (3.41)	34.5
50	89.9 (0.448)	40.10	14.0 (2.8)	31.3
40	80.6 (0.402)	46.24	12.7 (2.55)	31.6
33	60.4 (0.301)	59.75	12.5 (2.5)	41.5
29	40.9 (0.204)	72.72	12.2 (2.45)	59.8
25	30.3 (0.151)	79.81	9.1 (1.83)	60.3
22.5	19.9 (0.099)	86.76	6.1 (1.22)	61.6
20	10.2 (0.051)	93.18	3.0 (0.61)	58.8

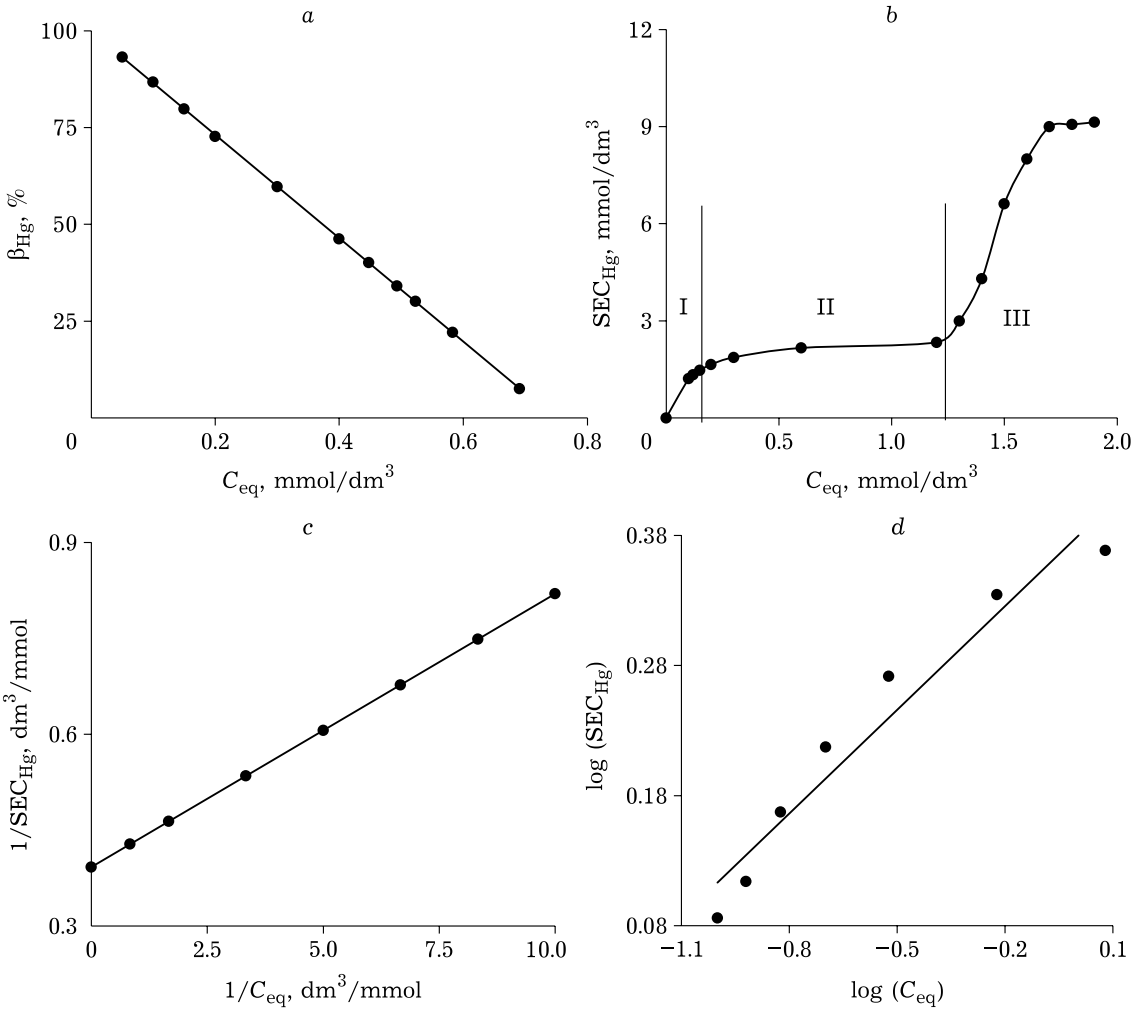

Fig. 1. Dependence of the degree of mercury recovery (β_{Hg}) from solution (*a*) and the static exchange capacity (SEC) of Lewatit MP 68 (*b*–*d*) on the equilibrium concentration of mercury (C_{eq}).

$1/C_{eq}))^2]$), where Q_s is the limiting amount of sorbed substance per unit mass/volume of the ion-exchange material (LSEC) or Langmuir constant; K_{ads} is adsorption constant; β is recovery of the sorbtive; $\varepsilon = RT \ln(1 + 1/C_{eq})$ is Polanyi potential (kJ/mol) depicting the isothermal work spent to transfer one mole of the sorbtive from the volume of the equilibrium solution to sorbent surface.

Dubinin–Radushkevich model, or the micropore volume filling theory (MVFT), is elaborated on the basis of Polanyi's theory of stage-by-stage adsorption [26]. According to MVFT, after primary filling of the functional centres of the resin, sorptive binding by the sorbent proceeds according to the mechanism of the formation of intermolecular structures under the action of physical adsorption forces. The application of the mathematical tools of MVFT is admitted with respect to the sorption of sorptive particles from the liquid phase into the polymer sorbent phase.

It is possible that in the region of high equilibrium concentrations, as well as under the conditions of rather long-term exposure of the ion-exchange resin in the model solution, the contribution from physical adsorption in total into the sorption process becomes increasingly significant. This causes an increase in the exchange capacity of the ion-exchange material, observed in the isotherm. Since this mechanism is due to the action of molecular forces and its effect on the process under dynamic conditions will be insignificant, within the framework of the present investigation the consideration was limited to sorption process with the application of classical interaction models of the type of sorbent – sorbate and sorbate – sorbate.

For low degree of resin filling with the sorbate ($C_{eq} \leq 0.4$ mmol/dm^3), distribution coefficient K_{distr} decreases from 58.8 to 31.6, however, with an in-

TABLE 3

Characteristics of mercury sorption on Lewatit MP 68

Langmuir model			Freundlich model		
Q_s, mmol/dm^3	K_{ads}, dm^3/mmol	R^2	K_s	n	R^2
2.55	$1.69 \cdot 10^{-2}$	0.99	2.39	0.27	0.94

crease in sorbability and the formation of sorbate structures (C_{eq} = 0.448–0.691 mmol/dm^3), K_{distr} values increase from 31.3 to 81.5 (see Table 2). The degree of mercury recovery from solution (β, %) is inversely proportional to the residual equilibrium concentration of the metal and corresponds to the linear equation: $\beta = -133.5C_{eq} + 99.81$ (see Fig. 1, *a*). By means of the graphical solution of the isotherm of mercury sorption from solutions (see Fig. 1, *c*, *d*), we determined Langmuir constant (Q_s, mmol/dm^3); the parameter characterizing the affinity of the ion-exchange material to the element to be adsorbed (K_{ads}, dm^3/mmol); constants K_s and n (Table 3); distribution constant K_{distr} (see Table 2). The isotherm itself is rather well described by Langmuir and Freundlich equations (see Table 3), which is evidenced by the high determination coefficient (R^2 is equal to 0.94 and 0.99, respectively).

The quantitative characteristics of mercury sorption depending on the time (τ) of contact with the resin (L/S = 100) and temperature (T) are presented in Table 4 and in Fig. 2. With an increase in the time of interaction τ = 1800 → 21 600 s and variation of solution temperature (T = 298/333 K), the recovery degree increases (β = 2.73 → 12.19/3.33 → 13.4 %), so does the distribution coefficient (K_{distr} = 2.82 → 13.91/3.46 → 15.51). The dependence of SEC on the time of mercury sorption at a temperature of 298 and 333 K is described by equations: $SEC_{298} = -3 \cdot 10^{-8}\tau^2 + 0.001\tau + 0.291$ (R^2 = 0.994) and $SEC_{333} = -3 \cdot 10^{-8}\tau^2 + 0.001\tau + 0.546$ (R^2 = 0.985), respectively. The integral sorption kinetic curves are presented in Fig. 2, *b*, where $F = \alpha_\tau/\alpha_\infty$ is relative sorption degree, equal to the ratio of sorptive concentration at the moment τ (α_τ) and at achieving the equilibrium (α_∞). The obtained dependences allow us to conclude that an increase in temperature somewhat increases the degree of mercury ion sorption. The time necessary for the equilibrium concentrations of mercury in solution and the resin phase to be established (α_∞) remains almost unchanged ~6 h within temperature range 298–333 K.

The experimental data were analyzed to reveal the possibility for internal and external diffusion processes to take place, and chemical reactions to occur during mercury sorption [27, 28]. The curves of the dependence $-\ln(1 - F) = f(\tau)$ at different temperatures are shown in Fig. 2, *c*. Initially (at small F) the dependence is linear and can be approximated by equation $\ln(1 - F) = -\gamma\tau$, where γ is the rate constant of film diffusion. This equation characterizes the external diffusion processes, when sorption rate is determined by ion distribution in the liquid film surrounding resin particles. At a definite degree of resin filling and with an increase in F, sorption curves lose their linearity (kinks appear) as a consequence of an increase in the fraction of mass transfer in the structure of ion exchange material during the sorption process. The simultaneous occurrence of the stages of external (film) and internal (gel) diffusion is the evidence of the mixed-diffusion sorption mode [29].

At the initial stage of sorption, the direct proportionality in the coordinates $F - \tau^{0.5}$ is evidence that internal diffusion is the stage limiting sorption in general (see Fig. 2, *d*).

The coefficient of gel diffusion of metal ions (D_g, m^2/s) and rate constants of internal diffusion (B, s^{-1}) were calculated using equations:

$D_g = (\pi F^2 r_0^2)/36\tau$

$B = (D_g\pi^2)/r_0^2$

TABLE 4

Dependence of Hg recovery on process duration at a temperature of 298/333 K

τ, s	C_{eq}, mmol/dm^3	β, %	Q_{sorb} (SEC), mmol/dm^3	$K_{distr} = Q_{distr}/C_{eq}$
1800	0.727/0.723	2.73/3.33	2.05/2.51	2.82/3.46
3600	0.708/0.698	5.33/6.66	4.02/5.03	5.65/7.16
7200	0.683/0.673	8.66/10.00	6.51/7.52	9.52/11.14
10 800	0.667/0.659	10.66/11.86	8.03/8.91	11.99/13.51
14 400	0.659/0.650	11.86/13.07	8.89/9.78	13.51/15.08
18 000	0.658/0.649	12.05/13.27	9.04/9.95	13.74/15.33
21 600	0.657/0.648	12.19/13.40	9.14/10.05	13.91/15.51

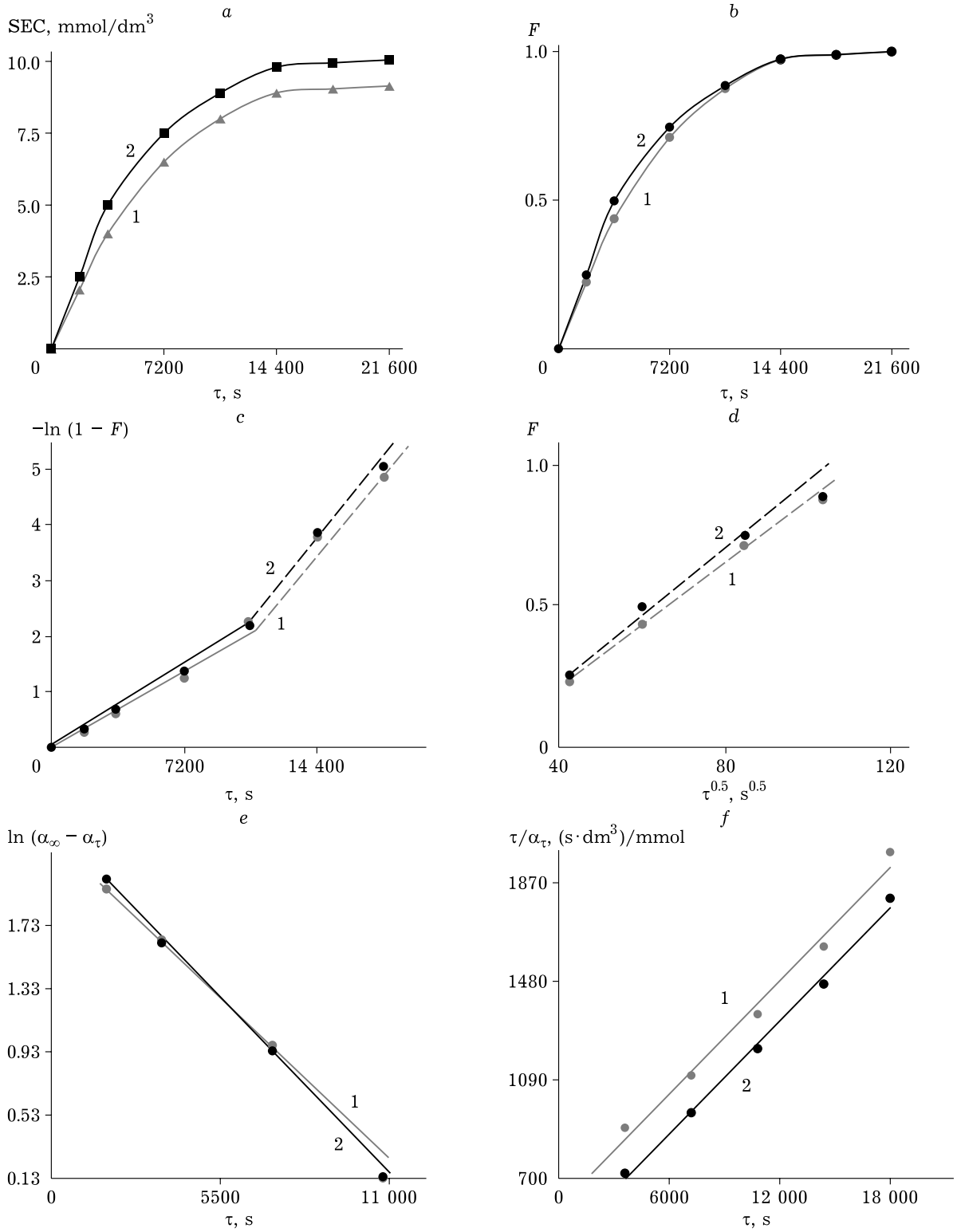

Fig. 2. Dependences of the static exchange capacity (SEC) on the time (τ) of sorption (*a*), kinetic curves of mercury sorption in different coordinates (*b*–*f*) on Lewatit MP 68 at a temperature of 298 (*1*) and 333 K (*2*), where $F = \alpha_\tau/\alpha_\infty$ is relative degree of sorption, equal to the ratio of the sorptive concentration at the moment τ (α_τ) and after having achieved the equilibrium (α_∞).

TABLE 5

Mercury diffusion coefficients and rate constants

T, K	D_g, m^2/s	γ, s^{-1}	B, s^{-1}	k_g, mmol/(dm^3 · s$^{0.5}$))
298	$3.39 \cdot 10^{-13}$	$1.6 \cdot 10^{-4}$	$4.58 \cdot 10^{-5}$	$6.7 \cdot 10^{-2}$
333	$4.38 \cdot 10^{-13}$	$1.9 \cdot 10^{-4}$	$5.92 \cdot 10^{-5}$	$8.3 \cdot 10^{-2}$

where $r_0 \approx 2.7 \cdot 10^{-4}$ m is the radius of Lewatit MP 68 grains.

The amount of sorbed ions in the internal diffusion process is expressed by equation $F\alpha_\infty = k_g\tau^{0.5}$ and presented in Table 5, where k_g is the rate coefficient of internal diffusion, mmol/(dm^3 · s$^{0.5}$).

According to the data presented in Table 5, the rate constants of external diffusion (γ = (1.6–1.9) · 10^{-4} s^{-1}) are approximately 3 times higher than the rate constants of internal diffusion (B = (4.58–5.92) · 10^{-5} s^{-1}). Along with constants γ and B, the values of coefficients D_g and k_g slightly increase (~25 %) with temperature rise within the range 298–333 K.

To reveal the contribution from the stage of chemical interaction during mercury sorption on Lewatit MP 68, we used the models: pseudo-first order, pseudo-second order, modified second order, and Elovich [30, 31]. The kinetic curves of the models of pseudo-first and pseudo-second order in the linear form are represented as the inversely proportional $\ln(\alpha_\infty - \alpha_\tau) - \tau$ (see Fig. 2, *e*) and directly proportional $(\tau/a_\tau) - \tau$ dependences, respectively (see Fig. 2, *f*). The values of parameters in the models of pseudo-first and pseudo-second order are listed in Table 6.

The models of modified second order and Elovich were not considered because, judging from determination coefficient (R_i^2), they provided lower accuracy in the description of experimental data than the models of pseudo-first and pseudo-second order.

It is shown that the kinetic equations of the pseudo-first and pseudo-second order models provide satisfactory description of experimental data ($R_i^2 > 0.98$), and that the difference between determination coefficients for the dependences $\ln(\alpha_\infty - \alpha_\tau) - \tau$ and $\tau/\alpha_\tau - \tau$ is not large.

The equation of pseudo-first order model $\ln(\alpha_\infty - \alpha_\tau) = \ln\alpha_\infty - k_1\tau$ is identical to the equation for film diffusion $\ln(1 - F) = -\gamma\tau$. Film thickness and size of ionite particles determine the rate of sorptive diffusion in the film. In the case if the sorption process is limited by the chemical reaction between functional groups of the ionite and the sorbate, the rate of sorptive recovery depends on temperature and on the concentration of the element to be sorbed. So, in the case when sorption kinetics are described by the pseudo-first order model, sorbent – sorbate interaction dominates. The chemical reaction of counter-ion exchange, limiting sorption process, is taken into account in both modes: pseudo-first and pseudo-second order.

In the case of the active interaction of sorbate ions with each other, the interaction of the functional group of ionite with the element to be extracted is described by the second-order equation [30]. So, the stage of chemical interaction of mercury ions with the functional groups of the sorbent and with each other makes a contribution into the total process rate.

The apparent activation energy (ΔE, see Table 6) may be determined through the calculation method using equation

$$\Delta E = [R \ln(k_{i1}/k_{i2}) \cdot T_1T_2]/(T_1 - T_2)$$

To calculate the thermodynamic characteristics of adsorption of the equilibrium state (ΔG^{eq}, ΔH^{eq}, ΔS^{eq}), we used the equations of isotherm and isobar in the integral form:

$$\Delta G^{eq} = -RT \ln K_{eq}$$

$$\Delta G^{eq} = \Delta H^{eq} - T\Delta S^{eq}$$

$$\ln K_{eq} = -\Delta H^{eq}/RT + \Delta S^{eq}/R$$

where K_{eq} is equilibrium constant.

$$SEC_0/SEC_\infty = (1 + K_{eq})/K_{eq}$$

$$K_{eq} = SEC_0/(SEC_\infty - SEC_0)$$

where SEC_0 and SEC_∞ (LSEC) are exchange capacities of the adsorbent for the formation of adsorbate monolayer and total exchange capacity, respectively (Fig. 3).

TABLE 6

Parameters of the kinetic models of mercury ion sorption

T, K	α_∞, mmol/dm^3	Pseudo-first order			Pseudo-second order		
		k_1, s^{-1}	R_1^2	ΔE, kJ/mol	k_2, s^{-1}	R_2^2	ΔE, kJ/mol
298	9.14	$2.30 \cdot 10^{-4}$	0.996	0.7	$1.43 \cdot 10^{-1}$	0.986	11.8
333	10.05	$2.09 \cdot 10^{-4}$	0.996	0.7	$2.36 \cdot 10^{-1}$	0.995	11.8

Within temperature range 298–333 K, for mercury sorption on Lewatit MP 68 resin, the following values of thermodynamic functions were obtained: $-\Delta G^{eq}$ = 2.35–2.99 kJ/mol; ΔH^{eq} = 3.1 kJ/mol; ΔS^{eq} = 18 J/(mol · K). The energy components of equilibrium state adsorption are positive ($\Delta H^{eq} > 0$), which is characteristic of endothermic process; small values ($\Delta H^{eq} < 10$ kJ/mol) indirectly point to the prevalence of diffusion mechanism in the physical adsorption of mercury ions. Entropy change during adsorption in the equilibrium state is positive ($\Delta S^{eq} > 0$) due to disordering of water dipoles during the interaction of mercury ions with the functional groups of Lewatit MP 68 resin.

During experiments on mercury sorption under dynamic conditions, the initial solution containing 0.046–0.99 g/dm^3 Hg was passed at the volume flow rate v = 2–5 h^{-1} through a weighted portion 1–10 g of Lewatit MP 68. As a result, it was determined that the dynamic exchange capacity of the resin with respect to mercury DEC_{Hg} = 260–270 g/dm^3; specific volume of the solution with respect to resin volume for its saturation in the dynamic mode V_{sol}/V_{sorb} = 3500–3800; content of the elements in saturated resin, %: Hg ~26.0, Se <1.0.

Introduction of the sorption technology of the purification of technological solutions from mercury in the chemical-metallurgical works instead of previously used mercury cementation on Al powder, the annual economic effect of ~3.5 mln roubles was obtained.

CONCLUSIONS

1. On the basis of experimental data, the sorption isotherm was plotted for the anion complexes of mercury on Lewatit MP 68 resin. Regions I–III may be distinguished in the isotherm, corresponding to the applicability of models: I – Henry ($Q_{sorb} = K_{ads}C_{eq}$); II – Langmuir ($C_{eq}/Q_{sorb} = C_{eq}/Q_s + 1/K_{ads}Q_s$); III – Dubinin–Radushkevich ($Q_{sorb} = Q_s \exp[-(K_{ads}/\beta^2)(RT \ln(1 + 1/C_{eq}))^2]$), where Q_{sorb} is the amount of sorbed substance per unit mass/volume of the ion exchange material (SEC); Q_s is the limiting amount of the sorbed substance per unit mass/volume of the ion exchange material (LSEC), or Langmuir constant; K_{ads} is the equilibrium adsorption constant; C_{eq} is the equilibrium concentration of the sorbtive; β is sorbtive recovery; $\varepsilon = RT \ln(1 + 1/C_{eq})$ is Polanyi potential (kJ/mol), depicting isothermal work of the transfer of one mole of sorbtive from the volume of the equilibrium solution to sorbent surface; $R = 8.314 \cdot 10^{-3}$ is the universal gas constant, kJ/(mol · K); T is absolute temperature, K.

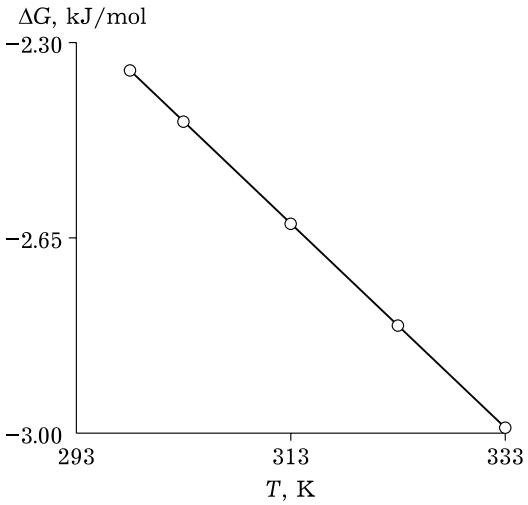

Fig. 3. Dependence of free Gibbs energy (ΔG) on temperature for mercury sorption on Lewatit MP 68 resin.

2. In the case of the low degree of resin filling with the sorbate ($C_{eq} \le 0.4$ mmol/dm^3), distribution constant K_{distr} decreases from 58.8 to 31.6; while the sorption ability increases and sorbate structures are formed (C_{eq} = 0.448–0.691 mmol/dm^3), K_{distr} values increase from 31.3 to 81.5.

3. The degree of mercury recovery from solution (β, %) is inversely proportional to the residual equilibrium concentration of the metal and corresponds to the linear equation: $\beta = -133.5C_{eq} + 99.81$.

4. With an increase in the time of interaction (τ = 1800 → 21 600 s) and variation of solution temperature (T = 298/333 K), the degree of recovery increases (β = 2.73 → 12.19/3.33 → 13.4 %) along with distribution coefficient (K_{distr} = 2.82 → 13.91/3.46 → 15.51).

5. At the initial stage of the mercury sorption process, the occurrence of the directly proportional dependence in the coordinates $F - \tau^{0.5}$ provides evidence that process rate is determined by the internal diffusion stage.

6. At a definite degree of resin filling and with an increase in F, sorption curves lose their linearity (kinks appear) as a consequence of an increase in the fraction of mass transfer in the structure of the ionite during sorption. The simultaneous occurrence of the external (film) and internal (gel) diffusion is the evidence of the mixed-diffusion mode of sorption.

7. The energy components of the adsorption of equilibrium state have positive are positive ($\Delta H^{eq} > 0$), which is characteristic of the endothermic process; small values ($\Delta H^{eq} < 10$ kJ/mol) indirectly

point to the prevalence of diffusion mechanism of physical adsorption of mercury ions.

8. Entropy change during adsorption in the equilibrium state is positive ($\Delta S^{eq} > 0$) as a consequence of disordering of water dipoles during the interaction of mercury ions with the functional groups of Lewatit MP 68 resin.

9. In the experiments on mercury sorption under dynamic conditions, initial solution 0.046–0.99 g/dm^3 Hg was passed through the weighted portion 1–10 g of Lewatit MP 68 with the volume flow rate of v = 2–5 h^{-1}. Finally, it was established that the dynamic exchange capacity of the resin with respect to mercury DEC_{Hg} = 260–270 g/dm^3; specific volume of the solution with respect to resin volume for its saturation in the dynamic mode V_{sol}/V_{sorb} = 3500–3800; element content in saturated resin is, %: Hg ~26.0; Se <1.0.

10. The introduction of sorption technology of the purification of technological solutions from mercury in the chemical-metallurgical works instead of the previously used mercury cementation on Al powder, the annual economic effect of ~3.5 mln roubles was achieved.

REFERENCES

1 Yang S., Li Z., Yan K., Zhang X., Xu Z., Liu W., Liu Z., Liu H., Removing and recycling mercury from scrubbing solution produced in wet nonferrous metal smelting flue gas purification process, *J. Environ. Sci.*, 2021, Vol. 103, P. 59–68.

2 Fabre E., Rocha A., Cardoso S. P., Brandão P., Vale C., Lopes C. B., Pereira E., Silva C. M., Purification of mercury-contaminated water using new AM-11 and AM-14 microporous silicates, *Sep. Purif. Technol.*, 2020, Vol. 239, Art. 116438.

3 Ponomarev A. V., Bludenko A. V., Makarov I. E., Pikaev A. K., Kim D. K., Kim Y., Han B., Combined electron-beam and adsorption purification of water from mercury and chromium using materials of vegetable origin as sorbents, *Radiat. Phys. Chem.*, 1997, Vol. 49, No. 4, P. 473–476.

4 Zhang B., Petcher S., Gao H., Yan P., Cai D., Fleming G., Parker D. J., Chong S. Y., Hasell T., Magnetic sulfur-doped carbons for mercury adsorption, *J. Colloid Interface Sci.*, 2021, Vol. 603, P. 728–737.

5 Pang X., Liu W., Xu H., Hong Q., Cui P., Huang W., Qu Z., Yan N., Selective uptake of gaseous sulfur trioxide and mercury in ZnO-CuS composite at elevated temperatures from SO_2-rich flue gas, *Chem. Eng. J.*, 2022, Vol. 427, Art. 132035.

6 Xin F., Xiao R., Zhao Y., Zhang J., Surface sulfidation modification of magnetospheres from fly ash for elemental mercury removal from coal combustion flue gas, *Chem. Eng. J.*, 2022, Vol. 436, Art. 135212.

7 Teng H., Altaf A. R., Elemental mercury (Hg^0) emission, hazards, and control: A brief review, *J. Hazard. Mater. Adv.*, 2022, Vol. 5, Art. 100049.

8 Ji Z., Huang B., Gan M., Fan X., Wang Y., Chen X., Sun Z., Huang X., Zhang D., Fan Y., Recent progress on the clean and sustainable technologies for removing mercury from typical industrial flue gases: A review, *Process Safety and Environmental Protection*, 2021, Vol. 150, P. 578–593.

9 Jia T., Luo F., Wu J., Chu F., Xiao Y., Liu Q., Pan W., Li F., Nanosized Zn-In spinel-type sulfides loaded on facet-oriented CeO_2 nanorods heterostructures as Z-scheme photocatalysts for efficient elemental mercury removal, *Sci. Total Environ.*, 2022, Vol. 813, Art. 151865.

10 Meng F., Umair M. M., Iqbal K., Jin X., Zhang S., Tang B., Rapid fabrication of noniridescent structural color coatings with high color visibility, good structural stability, and self-healing properties, *ACS Appl. Mater. Interfaces*, 2019, Vol. 11, No. 13, P. 13022–13028.

11 Anacleto A. L., Carvalho J. R., Mercury cementation from chloride solutions using iron, zinc and aluminium, *Miner. Eng.*, 1996, Vol. 9, No. 4, P. 385–397.

12 Gladyshev V. P., Levitskaya S. A., Filippova L. M., Analytical Chemistry of Mercury, Nauka, Moscow, 1974. (In Russ.).

13 Shen F., He S., Li J., Liu C., Xiang K., Liu H., Formation of sulfur oxide groups by SO_2 and their roles in mercury adsorption on carbon-based materials, *J. Environ. Sci.* (China), 2022, Vol. 119, P. 44–49.

14 Wadi V. S., Mittal H., Fosso-Kankeu E., Jena K. K., Alhassan S. M., Mercury removal by porous sulfur copolymers: Adsorption isotherm and kinetics studies, *Colloids and Surfaces A: Physicochemical and Engineering Aspects*, 2020, Vol. 606, Art. 125333.

15 Lennie A. R., Charnock J. M., Pattrick R. A. D., Structure of mercury(II)-sulfur complexes by EXAFS spectroscopic measurements, *Chem. Geol.*, 2003, Vol. 199, No. 3–4, P. 199–207.

16 Bell A. M. T., Charnock J. M., Helz G. R., Lennie A. R., Livens F. R., Mosselmans J. F. W., Pattrick R. A. D., Vaughan D. J., Evidence for dissolved polymeric mercury(II)-sulfur complexes, *Chem. Geol.*, 2007, Vol. 243, No. 1–2, P. 122–127.

17 Al-Jibori S. A., Al-Doori L. A., Al-Janabi A. S. M., Alheety M. A., Wagner C., Karadag A., Mercury(II) mixed ligand complexes of phosphines or amines with 2-cyanoamino thiophenolate ligands formed *via* monodeprotonation and carbon–sulfur bond cleavage of 2-aminobenzothiazole. X-ray crystal structures of $[Hg(SC_6H_4NCN)(PPh_3)]_2$ and $[Hg(SC_6H_4NCN)(Ph_2PCH_2PPh_2)]_2$, *Polyhedron*, 2021, Vol. 206, Art. 115349.

18 Shunin V. A., Sokolova I. S., Lebed A. B., Sorption purification of productive selenium-containing solutions from the admixtures of heavy metals, Abstracts, International Meeting "New Technologies of Beneficiation and Integrated Processing of Hard-to-Concentrate natural and Technogenic Mineral Raw Materials (Plaksin Readings 2011)", Verkhnyaya Pyshma, 19–24 September, 2011. P. 428–429. (In Russ.).

19 Habashi F., Metallurgical plants: How mercury pollution is abated, *Environ. Sci. Technol.*, 1978, Vol. 12, No. 13, P. 1372–1376.

20 Hylander I. D., Herbert R. B., Global emission and production of mercury during the pyrometallurgical extraction of nonferrous sulfide ores, *Environ. Sci. Technol.*, 2008, Vol. 42, No. 16, P. 5971–5977.

21 Yu M.-H., Yang H.-H., Gu Y.-C., Wang B.-H., Liu F.-C., Lin I. J. B., Lee G.-H., Formation of anionic NHC complexes through the reaction of benzimidazoles with mercury chloride. Subsequent protonation and transmetallation reactions, *J. Organomet. Chem.*, 2019, Vol. 887, P. 12–17.

22 Tugashov K. I., Gribanyov D. A., Dolgushin F. M., Smol'yakov A. F., Peregudov A. S., Klemenkova Z. S., Matvienko O. V., Tikhonova I. A., Shur V. B., Coordination chemistry of anticrowns. Isolation of the chloride complex

of the four-mercury anticrown {[(*o*,*o*′-$C_6F_4C_6F_4Hg)_4$]Cl}$^-$ from the reaction of *o*,*o*′-dilithiooctafluorobiphenyl with $HgCl_2$ and its transformations to the free anticrown and the complexes with *o*-xylene, acetonitrile, and acetone, *Organometallics*, 2017, Vol. 36, No. 13, P. 2437–2445.

23 Al-Amri A.-H. D., Fettouhi M., Wazeer M. I. M., Isab A. A., Synthesis, X-ray structure and ^{199}Hg, ^{77}Se CP MAS NMR studies on the first tris(imidazolidine-2-selone) mercury complex: {chloro-tris[*N*-methyl-2(3H)-imidazolidine-2-selone]mercury(II)}chloride, *Inorg. Chem. Commun.*, 2005, Vol. 8, No. 12, P. 1109–1112.

24 Hadjikakou S. K., Kubicki M., Synthesis, characterisation and study of mercury(II) chloride complexes with triphenylphosphine and heterocyclic thiones. The crystal structures of [(benzothiazole-2-thionato)(benzothiazole-2-thione)-(bis-triphenylphosphine) chloro mercury(II)] and [(μ_2-dichloro){(bis-pyrimidine-2-thionato)mercury(II)}{(bis-triphenylphosphine)mercury(II)}] at 100 K, *Polyhedron*, 2000, Vol. 19, No. 20–21, P. 2231–2236.

25 Pazderski L., Szlyk E., Wojtczak A., Kozerski L., Sitkowski J., Kamieński B., The crystal and molecular structures of *catena*[bis(μ_2-chloro)-(μ_2-pyridazine-*N*,*N*′)]cadmium(II) and *catena*[bis(μ_2-chloro)-(μ_2-pyridazine-*N*,*N*′)]mercury(II) and the solid-phase ^{13}C, ^{15}N NMR studies of Zn(II), Cd(II), Hg(II) chloride complexes with pyridazine, *J. Mol. Struct.*, 2004, Vol. 697, No. 1–3, P. 143–149.

26 Thomas J. M., Thomas W. J.,Principles and Practice of Heterogeneous Catalysis, Wiley, New York, 1997.

27 Saladze K. M., Pashkov A. B., Titov V. S., Ion-Exchange High-Molecular Compounds, Khimiya, Moscow, 1978. (In Russ.).

28 Saladze K. M., Kopylova-Valova V. D., Complex-Forming Ionites, Khimiya, Moscow, 1980. (In Russ.).

29 Kokotov Yu. A., Pasechnik V. A., Equilibrium and Kinetics of Ion Exchange, Khimiya, Leningrad, 1970. (In Russ.).

30 Ho Y. S., Ng J. C. Y., McKay G., Kinetics of pollutant sorption by biosorbents: Review, *Separ. Purif. Methods*, 2000, Vol. 29, No. 2, P. 189–232.

31 Cheung W. H., Ng J. C. Y., McKay G., Kinetic analysis of the sorption of copper(II) ions on chitosan, *J. Chem. Technol. Biotechnol.*, 2003, Vol. 78, No. 5, P. 562–571.